Published November 8, 2016

A family of membrane-shaping proteins at ER subdomains regulates pre-peroxisomal vesicle biogenesis

Amit S. Joshi,[1] Xiaofang Huang,[2,3] Vineet Choudhary,[1] Tim P. Levine,[4] Junjie Hu,[2,3,5] and William A. Prinz[1]

[1]Laboratory of Cell and Molecular Biology, National Institute of Diabetes and Digestive and Kidney Diseases, National Institutes of Health, Bethesda, MD 20892
[2]Department of Genetics and Cell Biology, College of Life Sciences and [3]Tianjin Key Laboratory of Protein Science, Nankai University, Tianjin 300071, China
[4]University College London Institute of Ophthalmology, London EC1V 9EL, England, UK
[5]National Laboratory of Macromolecules, Institute of Biophysics, Chinese Academy of Sciences, Beijing 100101, China

Saccharomyces cerevisiae contains three conserved reticulon and reticulon-like proteins that help maintain ER structure by stabilizing high membrane curvature in ER tubules and the edges of ER sheets. A mutant lacking all three proteins has dramatically altered ER morphology. We found that ER shape is restored in this mutant when Pex30p or its homologue Pex31p is overexpressed. Pex30p can tubulate membranes both in cells and when reconstituted into proteoliposomes, indicating that Pex30p is a novel ER-shaping protein. In contrast to the reticulons, Pex30p is low abundance, and we found that it localizes to subdomains in the ER. We show that these ER subdomains are the sites where most preperoxisomal vesicles (PPVs) are generated. In addition, overproduction or deletion of Pex30p or Pex31p alters the size, shape, and number of PPVs. Our findings suggest that Pex30p and Pex31p help shape and generate regions of the ER where PPV biogenesis occurs.

Introduction

The ER has a complex structure. It is composed of a single continuous membrane that is compartmentalized into perinuclear and peripheral ER. The peripheral ER extends from the outer nuclear membrane and forms a polygonal network of sheets and tubules that extends throughout the cell (Goyal and Blackstone, 2013). This structure is important for many of the critical cellular functions performed by the ER. Even though the functions of ER have been studied in detail, less is known about the mechanisms responsible for generating ER shape. The importance of studying ER morphogenesis is underscored by the fact that several diseases have been linked to defects in ER-shaping proteins (Westrate et al., 2015). ER shape is formed and maintained by the interactions of the ER with the cytoskeleton (Waterman-Storer and Salmon, 1998; Vedrenne et al., 2005; Ueda et al., 2010), homotypic ER–ER fusion by Sey1p/Atlastin and other fusogens (Hu et al., 2009; Anwar et al., 2012; English and Voeltz, 2013), and proteins that stabilize membrane curvature in the ER. These include Lnp1p/Lunapark, which stabilize the membrane curvature necessary to generate three-way junctions of ER tubules (Chen et al., 2012, 2015; Shemesh et al., 2014), and reticulon and reticulon-like proteins, which stabilize the high curvature of tubules and the edges of ER sheets (Voeltz et al., 2006; Hu et al., 2008; Shibata et al., 2008, 2010).

Reticulons and the reticulon-like proteins, called deleted in polyposis 1 (DP1) or receptor expression-enhancing proteins (REEP) in mammals and Yop1p in *Saccharomyces cerevisiae*, are highly abundant, integral ER membrane proteins found in all eukaryotic cells (Shibata et al., 2010). Even though these families share no sequence homology, they are thought to have two structural features that allow them to stabilize high curvature in the ER membrane. First, they have elongated hydrophobic domains predicted to form hairpins in the ER membrane. These domains, when present in large quantity, may either induce or stabilize membrane curvature, as these proteins reside primarily in the outer leaflet of the membrane (Voeltz et al., 2006; Shibata et al., 2010). Second reticulons and reticulon-like proteins have been proposed to form arc-shaped oligomers that scaffold the membrane (Shibata et al., 2008). Both families of proteins can directly shape membranes, as they are able to tubulate membranes when reconstituted into proteoliposomes (Hu et al., 2008). Overexpression of reticulons or DP1/Yop1p induces tubule formation, whereas depletion or elimination of these proteins results in a dramatic reduction in ER tubules and abnormal ER morphology (Voeltz et al., 2006; Tolley et al., 2008; Shibata et al., 2010). The abundance of reticulons and reticulon-like proteins determines the balance between ER tubules and ER

Correspondence to William A. Prinz: prinzw@helix.nih.gov

Abbreviations used: DysF, dysferlin; EPL, *Escherichia coli* polar lipids; LDAO, lauryldimethylamine-*N*-oxide; PPV, preperoxisomal vesicle; SC, synthetic complete; SE, standard error.

Supplemental Material can be found at:
/content/suppl/2016/11/07/jcb.201602064.DC1.html

The Rockefeller University Press $30.00
J. Cell Biol. Vol. 215 No. 4 515–529
https://doi.org/10.1083/jcb.201602064

Published November 8, 2016

sheets; increasing the amount of these proteins produces ER tubules at the expense of sheets (Shibata et al., 2010). Consistent with a role in stabilizing highly curved portions of the ER membrane, reticulons and reticulon-like proteins are enriched in ER tubules, the edges of ER sheets, and fenestrations of ER sheets (Dawson et al., 2009; Shibata et al., 2010).

The yeast *S. cerevisiae* has two reticulons (Rtn1p and Rtn2p) and one protein in the DP1/REEP/Yop1p family. Even though cells lacking all three of these proteins (*rtn1rtn2yop1Δ*) have dramatically altered ER structure, these cells still contain some ER tubules (West et al., 2011). Thus, yeast cells may have ER-tubulating proteins in addition to Rtn1p, Rtn2p, and Yop1p.

In this study, we sought to identify novel ER-shaping proteins by screening for proteins that, when overexpressed, restore ER structure in the yeast mutant *rtn1rtn2yop1Δ*. This screen identified two homologous proteins, Pex30p and Pex31p, which we show have previously unrecognized reticulon-like domains. Pex30p and Pex31p physically interact and have been implicated in peroxisome biogenesis (Vizeacoumar et al., 2004, 2006; Yan et al., 2008). Peroxisomes are single membrane-bound organelles ubiquitously present in eukaryotic cells and are required for several biosynthetic reactions such as hydrogen peroxide metabolism, β-oxidation, and the glyoxylate cycle (Van Veldhoven, 2010). The role of the ER in peroxisome biogenesis has remained controversial. Two findings suggest that the ER plays a role in peroxisome biogenesis. First, there is evidence that the peroxisomal membrane protein Pex3p and a few other integral membrane proteins are inserted into the ER and traffic in vesicles to peroxisomes (Hoepfner et al., 2005; Kim et al., 2006; Lam et al., 2010; van der Zand et al., 2010; Agrawal et al., 2011, 2016; Yonekawa et al., 2011). Second, the characterization of mutants lacking proteins needed for early steps of peroxisome biogenesis, like Pex3p and Pex19p in *S. cerevisiae*, revealed that these mutants are seemly devoid of peroxisomes but regenerate them when the missing *PEX* gene is reexpressed (Hoepfner et al., 2005; Haan et al., 2006; Motley and Hettema, 2007). This de novo peroxisome biogenesis was thought to initiate in the ER. However, this model was thrown into question by a recent study that revealed the existence of pre-peroxisomal vesicles (PPVs) in cells lacking Pex3p or Pex19p (Knoops et al., 2014). The PPVs had eluded detection because they were degraded by autophagy (Bellu et al., 2002; Williams and van der Klei, 2013); cells that lack Pex3p and Atg1p, which is required for autophagy, contain PPVs that can mature into functional peroxisome when Pex3p is reexpressed (Knoops et al., 2014). The origin of PPVs was not known.

In this study, we demonstrate that PPVs originate from the ER at regions that contain Pex30p and that Pex30p and Pex31p regulate the size and number of these PPVs. Our findings suggest that Pex30p and Pex31p shape and generate a subdomain of the ER in which PPVs bud from the ER.

Results

Overexpression of Pex30p or Pex31p restores ER shape in *rtn1rtn2yop1Δ* cells

S. cerevisiae cells lacking Rtn1p, Rtn2p, and Yop1p exhibit a dramatic reduction in ER tubules. However, these cells still contain some tubular ER, suggesting that there may be additional ER-shaping proteins (West et al., 2011). To identify novel ER-tubulating proteins, we performed a genetic screen (Fig. 1 A). The *rtn1rtn2yop1Δ* mutant exhibits only a modest growth defect but additional deletion of the *SPO7* gene in these cells renders them inviable (Dawson et al., 2009; Voss et al., 2012). Spo7p is part of phosphatase complex that regulates Pah1p, a key regulator of lipid metabolism (Santos-Rosa et al., 2005). Interestingly, cells missing Spo7p overproduce phospholipids and have an expanded ER (Campbell et al., 2006). We reasoned that overexpression of a novel ER-tubulating protein might restore viability to a strain lacking the reticulons and Spo7p (*rtn1rtn2yop1spo7Δ*). A conditional lethal *rtn1rtn2yop1spo7Δ* mutant was constructed that contained a plasmid with the *RTN1* gene and the counterselectable marker *URA3*. This strain is not viable in media containing 5-fluoroorotic acid, which kills cells expressing Ura3p (Fig. 1 B). The *rtn1rtn2yop1spo7Δ* mutant was transformed with a high-copy genomic library, and 32 suppressors were isolated from ∼18,000 transformants screened (Fig. 1 A). Six of the plasmids contained *PEX30* and one contained *PEX31*. Both the genes encode homologous proteins that physically interact and have been implicated in peroxisome biogenesis. Even though Pex30p and Pex31p are not essential for peroxisome biogenesis and function, they regulate peroxisome shape and abundance (Vizeacoumar et al., 2004). Both of the proteins also contain a dysferlin (DysF) domain, which has an unknown function (Vizeacoumar et al., 2004).

We confirmed that overexpression of Pex30p or Pex31p restores viability to *rtn1rtn2yop1spo7Δ* cells by cloning the genes encoding these proteins under the strong *RTN1* promoter in a high-copy (2μ) plasmid (Fig. 1 B). We determined whether the plasmids also corrected the ER morphology defect in *rtn1rtn2yop1Δ* cells (Fig. 1 C). In wild-type cells, the peripheral ER is largely tubular and appears discontinuous when focusing on the center of the cells, but in the *rtn1rtn2yop1Δ* mutant, the cortical ER forms large sheets and appears continuous when focusing on the center of cells. When Pex30p or Pex31p are overexpressed in *rtn1rtn2yop1Δ* cells, ER morphology looks like that of wild-type cells (Fig. 1 C), indicating that Pex30p and Pex31p may be ER-shaping proteins. Upon quantification of the number of cells with wild-type–like ER morphology, we found that Pex30p is able to restore ER structure in *rtn1rtn2yop1Δ* better than Pex31p (Fig. 1 D). We also used EM to confirm that overexpression of Pex30p restores the ER shape in *rtn1rtn2yop1Δ* cells (Fig. 1 E). The observation is specific to Pex30p and Pex31p because overexpression of Pex32p (a third DysF domain containing protein in yeast) or Pex3p (a protein required for peroxisome biogenesis) did not rescue the lethality of *rtn1rtn2yop1spo7Δ* (Fig. 1 B) or restore ER morphology (unpublished data). Together, these results indicate that Pex30p and Pex31p restore ER shape when overexpressed and may be novel tubulating proteins.

We wanted to rule out that Pex30p and Pex31p affect ER shape by altering lipid metabolism because the strain we used for the screen lacked Spo7p, a regulator of phospholipid abundance. It has previously been shown that the amount of phospholipid per cell increases dramatically in cells lacking Spo7p (Witkin et al., 2012). We found that overexpression of Pex30p or Pex31p in *spo7Δ* cells only moderately reduced phospholipid levels (Fig. S1), suggesting that these proteins do not affect ER shape by altering lipid metabolism.

Pex30p directly tubulates membranes in vitro and in cells

To determine whether the Pex30p, like the Rtn1p and Yop1p, can directly tubulate membranes, we tested whether purified

Published November 8, 2016

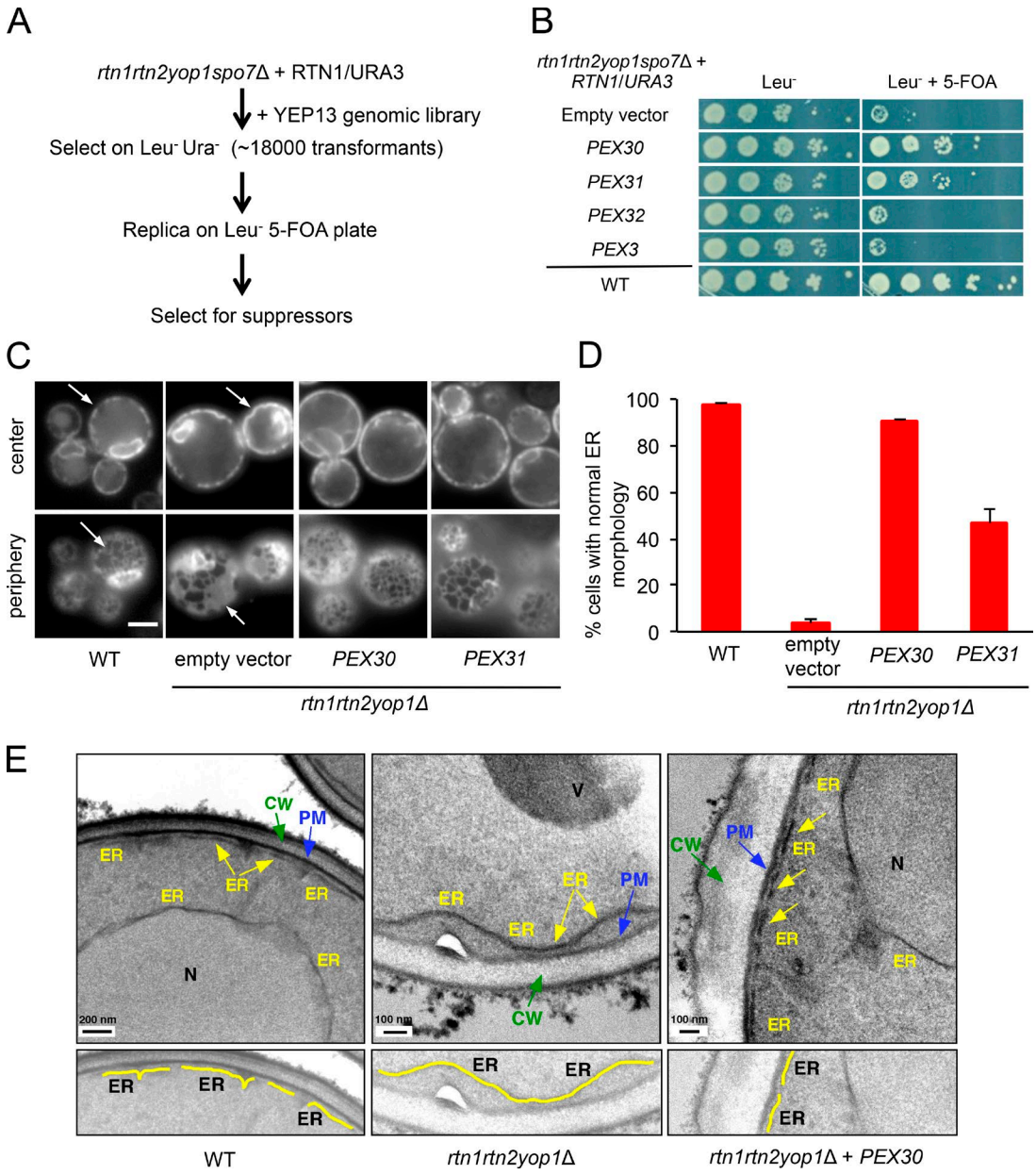

Figure 1. **Overexpression of Pex30p and Pex31p restores ER shape in *rtn1rtn2yop1Δ* cells.** (A) Schematic representation of the screen for genes that complement *rtn1rtn2yop1spo7Δ* cells. (B) The indicated strains were grown to mid-logarithmic growth phase, serially diluted, spotted onto plates that do or do not contain 5-fluoroorotic acid (5-FOA), and incubated at 30°C for 3 d. (C) Fluorescence microscopy images of strains expressing ss-RFP-HDEL focusing on the center (top) or periphery (bottom) of the cells. Arrows indicate normal cortical ER in wild-type (WT) and abnormal cortical ER in mutant. Bars, 3 µm. (D) Quantification of the experiment in C: Percentage of cells with normal ER morphology (mean ± SE; n = 3 biological replicates of at least 200 cells). (E) EM images of indicated strains. Yellow arrows indicate cortical ER; blue arrows, plasma membrane (PM); and green arrows, cell wall (CW). Bottom panel shows ER in yellow. Bars: (wild type) 200 nm; (*rtn1rtn2yop1Δ*) 100 nm. N, nucleus; V, vacuole.

Pex30p generates membrane tubules when reconstituted with pure phospholipids into proteoliposomes. Pex30p-Flag was overexpressed in *S. cerevisiae* and purified in the detergent lauryldimethylamine-*N*-oxide (LDAO) (Fig. 2 A). The purified protein was mixed with *Escherichia coli* polar lipids (EPL) in LDAO. Bio-Beads were added to remove the detergent, and the resulting proteoliposomes were analyzed by negative-stain EM. As expected and similar to Yop1p, small vesicles and short tubules were seen, both with a diameter of ∼20 nm (Fig. 2 B). Some tubules were also seen when the lipids were omitted (Fig. 2 C), presumably because of the presence of copurified natural lipids. In the absence of protein, round liposomes with heterogeneous size were generated (Fig. 2 D). We verified that Pex30p-Flag was reconstituted into liposomes by repeating the reconstitution using EPL containing a trace amount of a fluorescent lipid followed by sucrose-gradient centrifugation. Pex30p-Flag–containing tubules exhibited rapid sedimentation after the LDAO was removed (Fig. 2 E); a similar behavior in sucrose gradients was also observed when Yop1p was reconstituted into liposomes (Hu et al., 2008). We found that most of the lipid accompanied Pex30p-Flag in the gradients (Fig. 2 F), indicating that the protein was reconstituted into liposomes. These results indicate that Pex30p-Flag can be reconstituted into proteoliposomes and suggest that the protein induces membrane

Published November 8, 2016

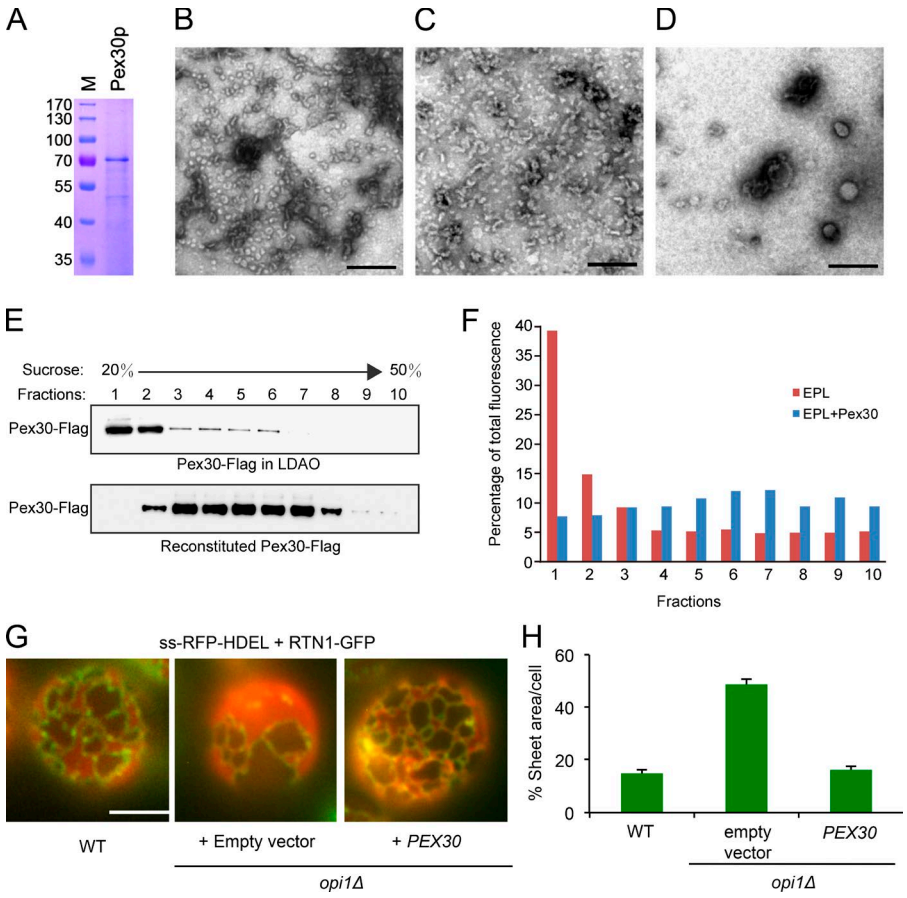

Figure 2. **Pex30p tubulates membrane in vivo and in vitro.** (A) Pex30p-Flag was purified from *S. cerevisiae* and analyzed by SDS-PAGE followed by staining with Coomassie blue. (B) Pex30p-Flag in LDAO was mixed with *EPL*, incubated with Bio-Beads for 4 h, and visualized by negative-stain EM. (C) As in B, but without EPL. (D) As in B, but without protein. Bars, 200 nm. (E) Pex30p in LDAO was subjected to sucrose density-gradient centrifugation before (top) or after incubation with EPL, a fluorescent phospholipid, and Bio-Beads to remove LDAO (bottom). Fractions were immunoblotted with an anti-Flag antibody. (F) Relative amount of fluorescent phospholipid in the fractions from the bottom panel of E (EPL + Pex30p) and an identical experiment without protein (EPL). (G) Fluorescence microscopy images of the periphery of wild-type (WT) and *opi1*Δ cells expressing Rtn1p-GFP (green) and ss-RFP-HDEL (red). Bar, 3 µm. (H) Quantification of the experiments in G. The relative area of ER sheets was determined from the area of ss-RFP-HDEL fluorescence that did not colocalize with Rtn1p-GFP fluorescence (mean ± SE; *n* = 16). M, molecular mass markers (in kD).

tubules in liposomes that are similar to those formed by purified Yop1p and Rtn1p.

We next determined the ability of Pex30p to tubulate ER membrane in vivo using a previously described assay (Shibata et al., 2010). This assay makes use of the fact that Rtn1-GFP localizes to ER tubules and the edges of ER sheets. In cells expressing both Rtn1-GFP and the ER luminal marker ss-RFP-HDEL, the percent of the peripheral ER sheet area is proportional to the area where Rtn1-GFP and ss-RFP-HDEL do not colocalize. In wild-type cells, ∼20% of the peripheral ER consists of sheets (Fig. 2, G and H; Shibata et al., 2010). In cells lacking the transcriptional regulator Opi1p (*opi1Δ*), phospholipids are overproduced, and the amount of sheets in the peripheral ER increases to ∼50% (Fig. 2, G and H; Shibata et al., 2010). The percent of sheets in the ER in *opi1Δ* cells is restored to near wild-type levels when Rtn1p is overexpressed (Shibata et al., 2010). We found that overexpression of Pex30p, similar to Rtn1p, increased the amount of tubular ER (Fig. 2, G and H), indicating that Pex30p tubulates the ER in cells. Our findings show that both in vitro and in cells, Pex30p and probably Pex31p tubulate ER membranes.

Pex30p and Pex31p are reticulon-like tubulating proteins

We next investigated whether Pex30p and Pex31p are functionally similar to reticulons. When Pex30p and Pex31p are overexpressed, they have a localization that is similar to that of the reticulons (Fig. 2 G); they are enriched in ER tubules and the edges of ER sheets (Fig. 3 A). This localization does not require the DysF domain because a truncated version of Pex30p that contains only the N-terminal 235 aa and lacks the DysF domain maintains a reticulon-like distribution in the ER (unpublished data).

Using the structure-based domain prediction program HHpred, we found that the N-terminal portions of Pex30p and Pex31p are similar to the membrane-shaping domains of reticulons (Fig. 3 B and Fig. S2). These domains contain a conserved tryptophan residue (Fig. 3 C). We reasoned that if mutating the conserved tryptophan residues in a reticulon and in Pex30p rendered the proteins nonfunctional, then they may shape membranes by a similar mechanism. To test this, we mutated the conserved tryptophan residues in Pex30p and Rtn2p to cysteine. Overexpression of the mutated Pex30p or Rtn2p under the strong *RTN1* promoter did not rescue the lethality of *rtn1rtn2yop1spo7Δ* cells (Fig. 3 D). In addition, the mutant proteins did not restore ER morphology in *rtn1rtn2yop1Δ* cells (Fig. 3 E). When we expressed the mutant Pex30p at high levels in yeast to purify it, the yield of full-length protein was significantly lower than that of wild-type protein (unpublished data), suggesting that the mutation may render Pex30p unstable. Although the mutant Pex30p was still able to generate some tubules in vitro, the protein was used at approximately five times higher concentration than wild type. Thus, mutation of the conserved tryptophan residue that is required for the function of Pex30p in cells may reduce the stability of the protein and its ability to tubulate membranes. Our findings suggest that the putative transmembrane regions at the N termini of Pex30p and Pex31p are reticulon-like domains.

Additional evidence that Pex30p and Pex31p are reticulon-like proteins was obtained by examining the genetic interaction

Published November 8, 2016

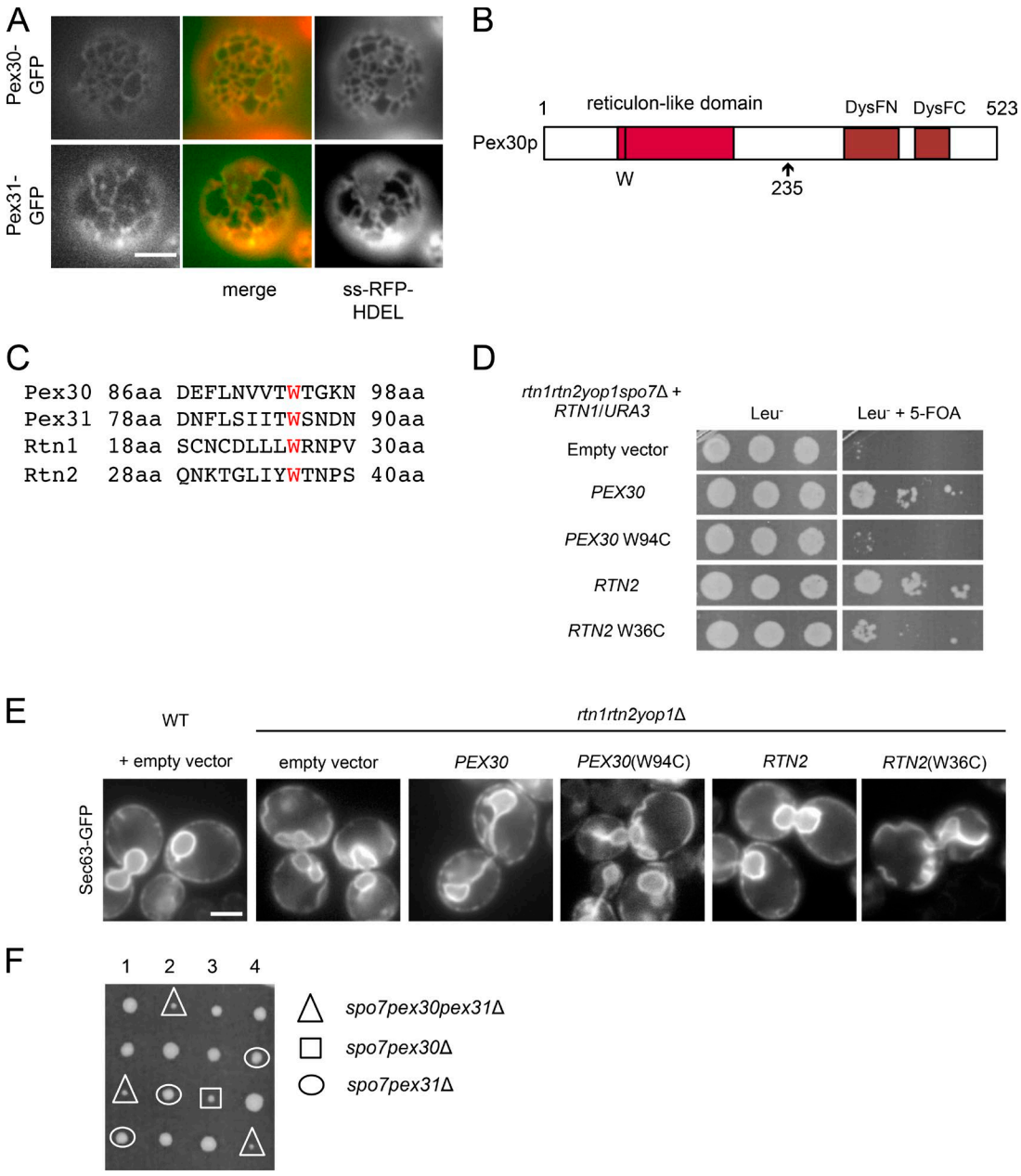

Figure 3. **Pex30p and Pex31p are reticulon like ER-shaping proteins.** (A) Fluorescence microscopy (FM) images of *rtn1rtn2yop1Δ* cells expressing ss-RFP-HDEL and Pex30-GFP or Pex31-GFP from high-copy plasmids. Bar, 3 µm. (B) Predicted domain architecture of Pex30p; reticulon-like domain was identified using HHpred. The DysF domain has two parts, DysFN and DysFC. (C) Conserved tryptophan shown in red in the aligned amino acid sequence of Rtn1p, Rtn2p, Pex30p, and Pex31p using HHpred. (D) Serial dilutions of cultures of the indicated strains as in Fig. 1 B. (E) FM images of cortical ER in the indicated strains expressing Sec63-GFP. Bar, 3 µm. (F) Heterozygous *spo7Δpex30Δpex31Δ* diploid cells were sporulated, and the haploid spores were separated and grown on plates. Genotypes of selected haploids are indicated. 5-FOA, 5-fluoroorotic acid.

of *PEX30* and *PEX31* with *SPO7*. We found that *pex30Δ* and *pex31Δ*, like *rtn1rtn2yop1Δ*, exhibit negative genetic interactions with *spo7Δ* (Fig. 3 F). The *pex30Δ* allele exhibits a strong genetic interaction with *spo7Δ*, whereas deletion of *PEX31* slightly exacerbates the growth defect of *spo7Δ* and *spo7pex30Δ* (Fig. 3 F). Collectively, our findings suggest that Pex30p and Pex31p are reticulon-like tubulating proteins.

Endogenous Pex30p localizes to subdomains of the peripheral ER

To further explore the role of Pex30p and Pex31p in tubulating the ER membrane, we investigated the localization of these proteins. Previous studies have indicated that Pex30p and Pex31p localize to both the ER and peroxisomes in *S. cerevisiae* and other yeast (Vizeacoumar et al., 2006; Yan et al., 2008; David et al., 2013). We sought to determine the localization of endogenous Pex30p and Pex31p fused to fluorescent proteins and were able to visualize endogenously expressed Pex30-GFP and Pex30-2xmCherry (Fig. 4 A) but Pex31-GFP was too dim to be visualized, presumably because of its low abundance. Pex30-2xmCherry was primarily localized to tubular ER and the edges of the ER sheets but was largely absent from the perinuclear ER (Fig. 4 A). However, unlike the reticulon proteins, Pex30-2xmCherry is not uniformly distributed on ER tubules

Published November 8, 2016

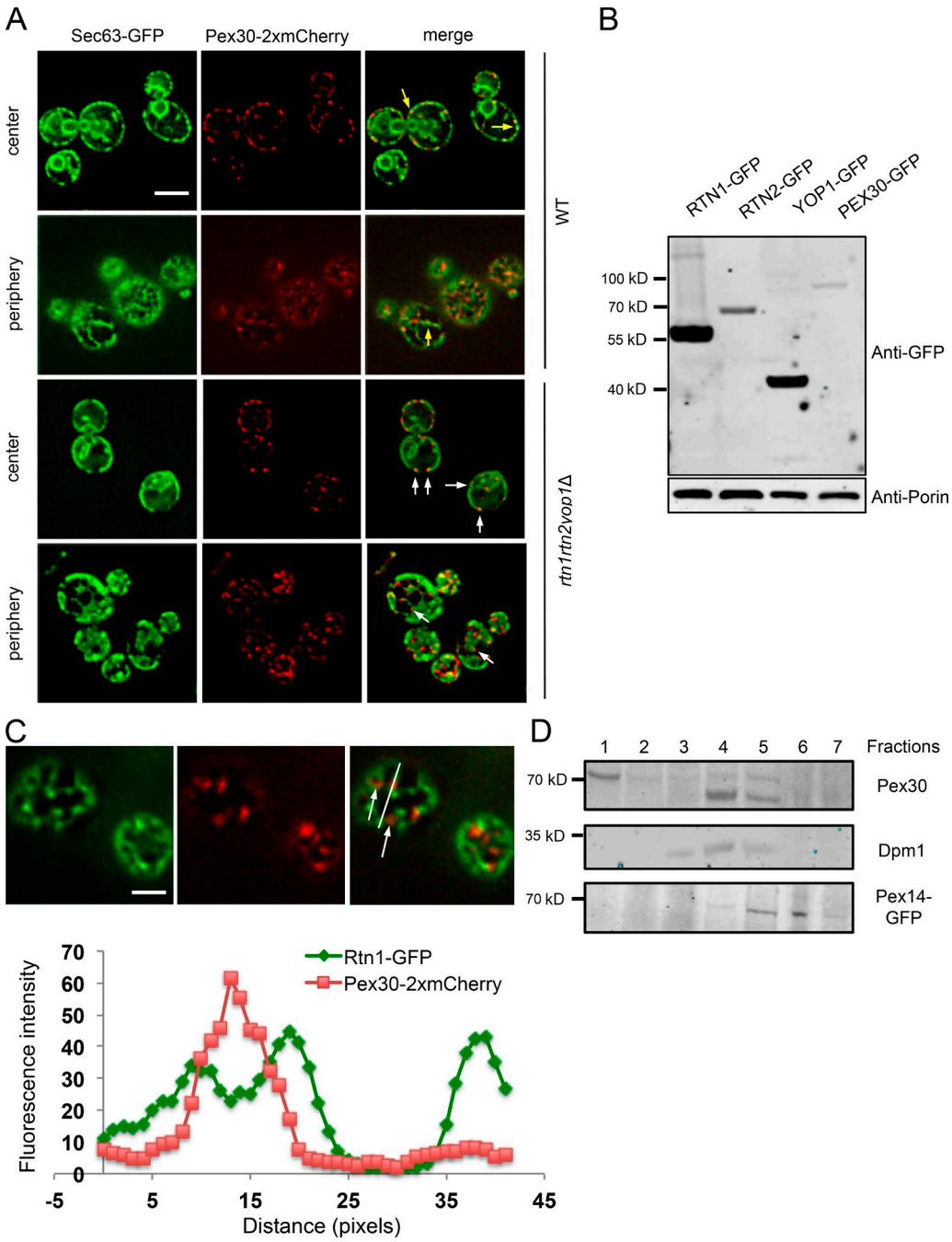

Figure 4. **Pex30p localizes to subdomains of the ER.** (A) Fluorescence microscopy (FM) images expressing endogenous Pex30-2xmCherry and Sec63-GFP focusing on the center or periphery of cells. Yellow arrows indicate Pex30-GFP subdomains in ER tubules, and white arrows indicate Pex30-GFP at the edges of ER sheets. Bar, 3 µm. (B) Immunoblots of whole-cell extracts from the indicated strains; equal amounts of protein were separated using 4–12% SDS-PAGE. (C) FM images (top) of cells expressing endogenous Pex30-2xmCherry and Rtn1-GFP. The intensity of the pixels was measured using ImageJ. Bar, 3 µm. The line profile graph (bottom) shows the pixel intensities for Pex30-2xmCherry (red) and Rtn1-GFP (green) along the line drawn across the cell as shown in the figure. (D) Cell lysate were fractionated by centrifugation on a Histodenz step gradient. Pex30p cofractionated with the ER marker Dpm1p. Pex14-GFP was used as a marker for peroxisomes.

and the edges of ER sheets but instead forms punctae in these regions (Fig. 4 A). Remarkably, we found that Pex30-2xmCherry localizes at the regions of ER tubules that are nearly devoid of Rtn1-GFP (Fig. 4 C), suggesting that Pex30p resides in subdomains of ER and may be the most abundant ER-shaping protein in these regions. To confirm the subcellular localization of Pex30p in the ER, we performed density-gradient centrifugation. Pex30p fractioned similarly to the ER protein Dpm1p and not Pex14-GFP (Fig. 4 D). Thus, Pex30p is an ER-resident protein and absent from peroxisomes in cells grown on glucose, which is consistent with a recent study (Mast et al., 2016).

Interestingly, we also found a modified form of Pex30p, with a higher molecular mass of ~70 kD, in the top fraction, suggesting that this modified form of Pex30p may reside in ER

Published November 8, 2016

associated with lipid droplets. Pex30p also localizes to regions of close contact between the nucleus and the vacuoles called the nuclear–vacuolar junction, especially in cells at stationary phase (unpublished data). As Pex30p was previously shown to physically interact with Pex31p (Vizeacoumar et al., 2004), we suspect that Pex31p is also present at ER subdomains.

Unlike the reticulons and Yop1p, Pex30p and Pex31p do not appear to play a significant role in shaping the ER because ER morphology was normal in a strain lacking both proteins (Fig. S3). In addition, elimination of Pex30p and Pex31p in the *yop1Δ* mutant does not exacerbate the ER morphology defect in these cells (Fig. S3). It seems likely that Pex30p and Pex31p only affect ER shape when they are overexpressed because the endogenous proteins are low abundance, whereas the reticulons and Yop1p are among the most abundant proteins in the ER membrane. Immunoblotting analysis indeed confirmed that endogenously expressed Pex30-GFP is much less abundant than the reticulons or Yop1p (Fig. 4 B). Thus, Pex30p and probably Pex31p may shape subdomains in ER tubes or the edges of sheets but are not abundant enough to alter ER shape globally unless they are overexpressed.

Rate of de novo peroxisome biogenesis decreases in cells lacking Pex30p and Pex31p

What are the functions of Pex30p and Pex31p in ER subdomains? Previous studies have suggested that Rtn1p, Rtn2p, and Yop1p as well as Pex30p play similar but poorly understood roles in de novo peroxisome biogenesis, which is thought to occur on the ER membrane (David et al., 2013). The rate of de novo synthesis of mature peroxisomes is commonly studied in cells in which the expression of Pex3p is controlled by a galactose-inducible promoter (*GAL1-PEX3*; David et al., 2013). We monitored the formation of mature peroxisomes in these cells using mCherry-SKL, which has a peroxisomal targeting sequence. This protein remains in the cytoplasm of cells without functional peroxisomes but is imported into the mature peroxisomes when they form. *GAL1-PEX3* cells grown in media with raffinose lack peroxisomes. When galactose is added to the medium, Pex3p production is induced, and de novo peroxisome biogenesis begins.

It has previously been shown that in *rtn1rtn2yop1Δ* mutant cells, the rate of de novo peroxisome biogenesis is faster than in wild-type cells (David et al., 2013), a result we confirmed (Fig. 5 A). This study also found that *pex30Δ* cells have an increased rate of de novo peroxisome biogenesis using a different assay (David et al., 2013). In contrast, we found that the rate of peroxisome synthesis in cells lacking Pex30p and Pex31p was lower than that of wild type (Fig. 5 A and Fig. S4). Furthermore, deletion of *PEX30* and *PEX31* in the *rtn1rtn2yop1Δ* mutant also decreased the rate of mature peroxisome biogenesis (Fig. 5 A and Fig. S4). Although Pex3p overproduction from the strong *GAL1* may affect peroxisome biogenesis, there did not seem to be any difference among the strains in the extent of peroxisome clumping or any indication of significant pexophagy, as indicated by GFP signal in vacuoles (Fig. S4). In addition, the difference in the rate of de novo biogenesis was not because of alteration in expression of Pex3p (Fig. 5 B). These findings confirm that Pex30p and Pex31p play roles in de novo biogenesis of peroxisomes but, surprisingly, suggest that their function may be different than that of the reticulons and Yop1p despite sharing similar membrane-shaping domains.

Pex30p and Pex31p play a role in PPV biogenesis

The role of ER in peroxisome biogenesis is not well understood. During de novo formation of peroxisomes, it is thought that PPVs bud from the ER and mature to form functional peroxisomes (Dimitrov et al., 2013; Agrawal and Subramani, 2016). We speculated that Pex30p and Pex31p might play roles in PPV biogenesis in the ER. Until recently, it was believed that cells lacking Pex3p were devoid of PPVs. However, it was found that these cells generate PPVs that are normally degraded by autophagy. About one to three PPVs were found in cells lacking Pex3p and Atg1p (*pex3atg1Δ*). The PPVs were found to harbor peroxisomal importomer complex proteins such as Pex14p and Pex13p (Rucktäschel et al., 2011). Thus, Pex14-GFP can be used to detect PPVs in *pex3atg1Δ* cells.

To determine the role of Pex30p and Pex31p in PPV generation, we deleted these genes in *pex3atg1Δ* cells expressing Pex14-GFP. We confirmed the presence of PPVs in *pex3atg1Δ* cells by colocalizing Pex14-GFP with Pex13-mCherry, another marker for PPVs (Fig. S5). Interestingly, deletion of *PEX30* or *PEX31* in *pex3atg1Δ* cells lead to a significant decrease in the number of PPVs per cell (Fig. 5 C). In contrast, *rtn1rtn2yop1pex3atg1Δ* cells had an increase in the number of PPVs (Fig. 5, C and D). Deletion of *PEX30* and *PEX31* in *rtn1rtn2yop1pex3atg1Δ* cells resulted in a reduction in the number of PPVs, indicating that Pex30p and Pex31p affect PPV biogenesis (Fig. 5, C and D). Interestingly, we found that expression of Pex30 under the strong *RTN1* promoter led to an increase in the mean number of Pex14-GFP punctae in *pex3atg1Δ* cells (1.56 ± 0.122 spots/cell). Accordingly, these findings suggest that Pex30p and Pex31p promote but are not required for PPV biogenesis.

Pex14p containing PPVs originate from the ER

To further investigate the role of Pex30p and Pex31p in PPV generation in the ER, we first needed a method to visualize the production of PPVs in the ER. We speculated that after Pex14-GFP is synthesized, it binds to the ER, and then PPVs containing Pex14-GFP bud from the ER. We first generated a *pex3atg1Δ* strain that expressed the ER marker ss-RFP-HDEL and endogenously expressed Pex14-GFP and found that ∼45% of Pex14-GFP puncta colocalize with the ER marker ss-RFP-HDEL (Fig. 6, A and B). This finding suggests that some Pex14-GFP puncta are not on vesicles but on regions of the ER, which we confirmed using immunogold EM (Fig. 6 C and see Fig. 8 B, I). These findings are consistent with a recent paper showing that a complex containing Pex14p can be found on the ER (Agrawal et al., 2016).

To determine whether newly synthesized Pex14p is initially on the ER and eventually leaves the ER in PPVs, we used a strain in which GFP-Pex14 is expressed by the regulatable *GAL1* promoter. We found that all newly formed GFP-Pex14 puncta initially colocalize with the ER (Fig. 6, D and E) and eventually appear to move away from the ER (Video 1). Together, these findings suggest that GFP-Pex14 is initially targeted to the ER and then exits the ER on newly formed PPVs.

Pex30p is enriched at sites of PPV production

Consistent with a role for Pex30p and Pex31p in PPV production, we found that the *pex30pex31pex3atg1Δ* has significantly more Pex14-GFP puncta on the ER (Fig. 6 B). We suspected

Published November 8, 2016

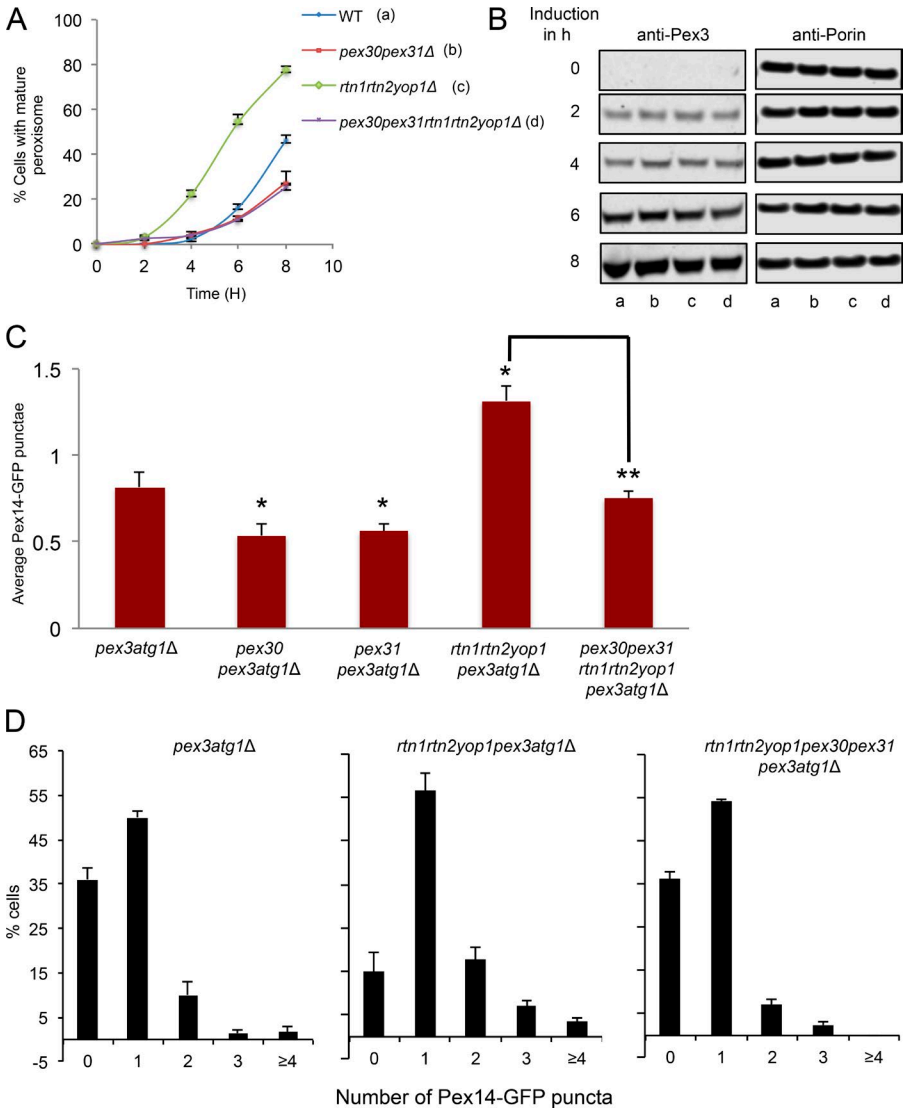

Figure 5. **Pex30p and Pex31p play a role in PPV biogenesis.** (A) Peroxisome biogenesis was induced as described in Materials and methods; graph shows percentage of cells containing mature peroxisomes at indicated time points after induction of Pex3p expression ($n = 3$). (B) Immunoblots of the strains in A with antibodies against Pex3p and anti-porin (as a loading control). (C) Mean number of Pex14-GFP puncta in the indicated strains; mean ± SE of three replicates, at least 100 punctae counted per replicate (*, $P < 0.05$; **, $P < 0.005$). (D) The results in C were regraphed to show the mean number of cells with the indicated number of Pex14-GFP punctae.

that Pex14-GFP puncta on the ER are less mobile than those in PPVs, and indeed, we found that Pex14-GFP puncta are significantly less mobile in *pex30pex31pex3atg1Δ* cells (Fig. 7 A). Together, these findings suggest that Pex30p and Pex31p promote PPV production in the ER.

If Pex30p plays a direct role in PPV production, then it might be enriched in regions of the ER where PPVs are generated. To test this, we expressed Pex14-GFP or Pex14-YFP in cells that also expressed Pex30-2xmCherry. We found that ∼33% of Pex14-GFP puncta colocalize with Pex30-2xmCherry on the ER (Fig. 7, B and C), a number that is similar to the 45% of Pex14-GFP puncta on the ER (Fig. 6 B). In contrast, Pex30-2xmCherry did not colocalize with the ER exit sites for COPII vesicles. We found that only 7% of Sec13-GFP puncta, a marker for these exit sites (Shindiapina and Barlowe, 2010), colocalized with Pex30-2xmCherry puncta (Fig. 7, B and C). These results suggest that the PPV exit sites containing Pex30p are distinct from the COPII exit sites marked by Sec13p. Thus, Pex30p, and probably Pex31p, are enriched in regions of the ER where PPV biogenesis occurs and may play direct roles in PPV production.

To confirm the localization of Pex30p at sites of PPV biogenesis, we sought to determine whether newly formed GFP-Pex14 punctae colocalize with Pex30p and then move away from the ER. We reasoned that if PPV biogenesis occurs at Pex30 sites in the ER, we would initially see a high degree of colocalization that would then decrease over time. To test this, we used a strain in which GFP-Pex14 expression is controlled by the *GAL* promoter (Fig. 7 E) and that also expresses Pex30-mCherry and lacks Pex3p and Atg1p. The colocalization of GFP-Pex14 and Pex30-mCherry was monitored over time after induction of GFP-Pex14 expression (Fig. 7 E). We found that the highest degree of colocalization occurred immediately after GFP-Pex14 induction and that colocalization subsequently decreased over time (Fig. 7 D). However, GFP-Pex14p is overexpressed at later time points (Fig. 7 E), and we cannot rule out that overexpression of GFP-Pex14p affects its targeting to Pex30p-containing subdomains of the ER. These findings are consistent with the idea that Pex14-containing PPVs form at regions of the ER containing Pex30p and then leave the ER.

Pex30p regulates the morphology of preperoxisomal vesicles

As Pex30p and Pex31p stabilize membrane curvature and may play roles in PPV biogenesis, we speculated that PPVs in cells lacking these proteins might have altered morphol-

Published November 8, 2016

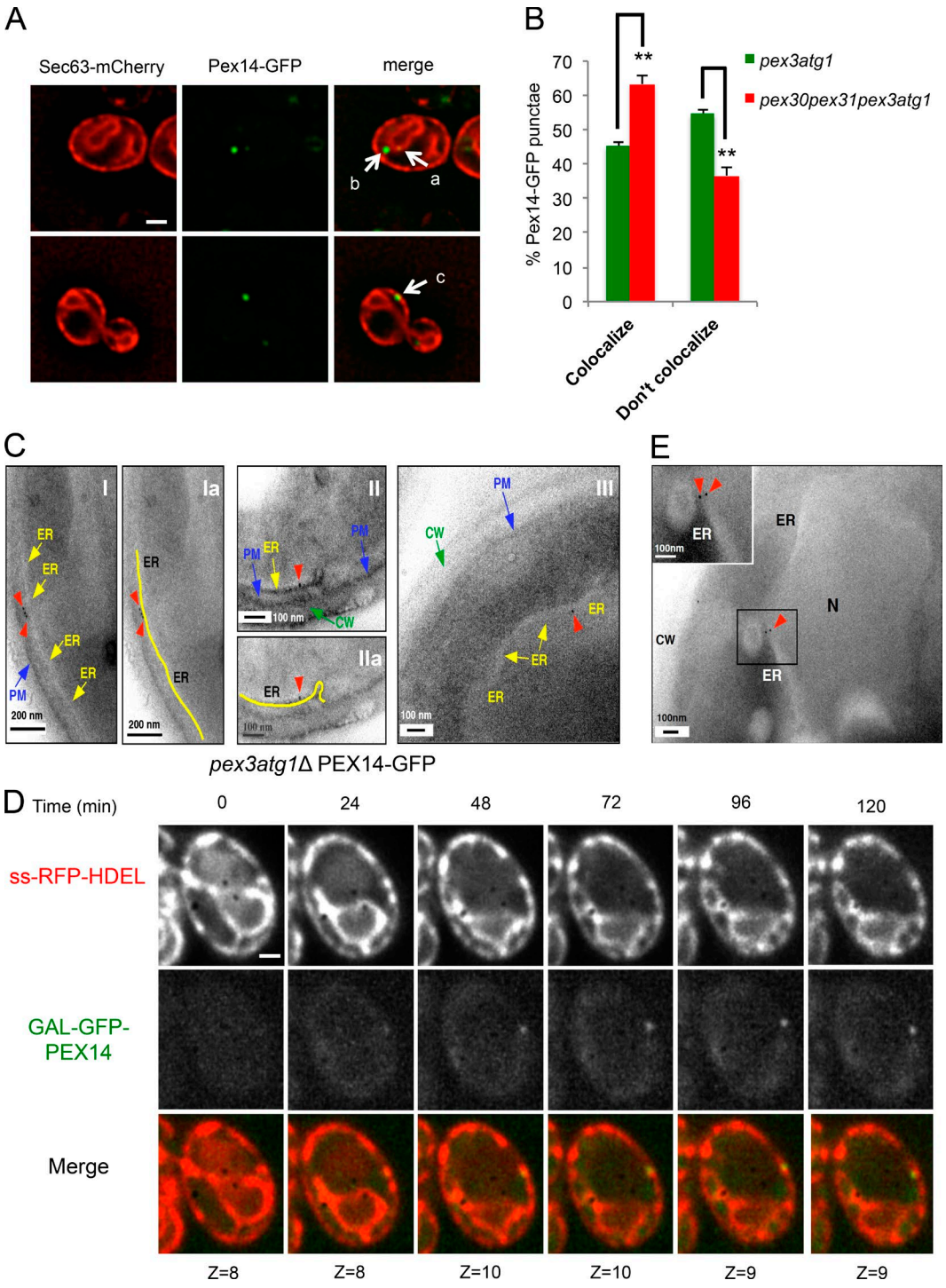

Figure 6. **Pex14-GFP containing PPVs originate in the ER.** (A) Fluorescence microscopy (FM) images of *pex3atg1*Δ cells expressing endogenously tagged Pex14-GFP and Sec63-mCherry expressed from a plasmid. Arrows indicate Pex14-GFP puncta that colocalize with the ER (a), do not colocalize with the ER (b), or associate with the ER (c). Stacks of five images with a step of size of 0.25 µm were taken and deconvolved; images from a single plane are shown. Bar, 3 µm. (B) Quantification of the experiment in A; colocalize = (a) + (c) and do not colocalize = (b). At least 50 Pex14-GFP punctae were counted for each strain (mean ± SE; $n = 3$; **, $P < 0.05$). (C) Immunogold EM images (I–III) of *pex3atg1*Δ cells expressing endogenously tagged Pex14-GFP using anti-GFP antibodies. Ia and IIa are cartoon depictions of I and II, respectively. Red arrowheads indicate the gold particle; green arrows, cell wall (CW); blue arrows, plasma membrane (PM); yellow arrows, ER. (D) Time-lapse FM images of *pex3atg1*Δ cells expressing ss-RFP-HDEL and GFP-Pex14 under the *GAL1* promoter. Cells were precultured in a medium with 2% raffinose, induced with 2% galactose for 15 min, shifted back to a medium with only 2% raffinose, and cells were visualized after 15 min (time = 0). Stacks of 10 images with a step of size of 0.25 µm were taken and deconvolved. Images from the indicated plane (z) are shown. Bar, 1 µm. (E) Immuno-EM of cells from D. Cells were grown as in D for 60 min after shifting back to medium with only 2% raffinose. Red arrowheads indicate gold particle.

Published November 8, 2016

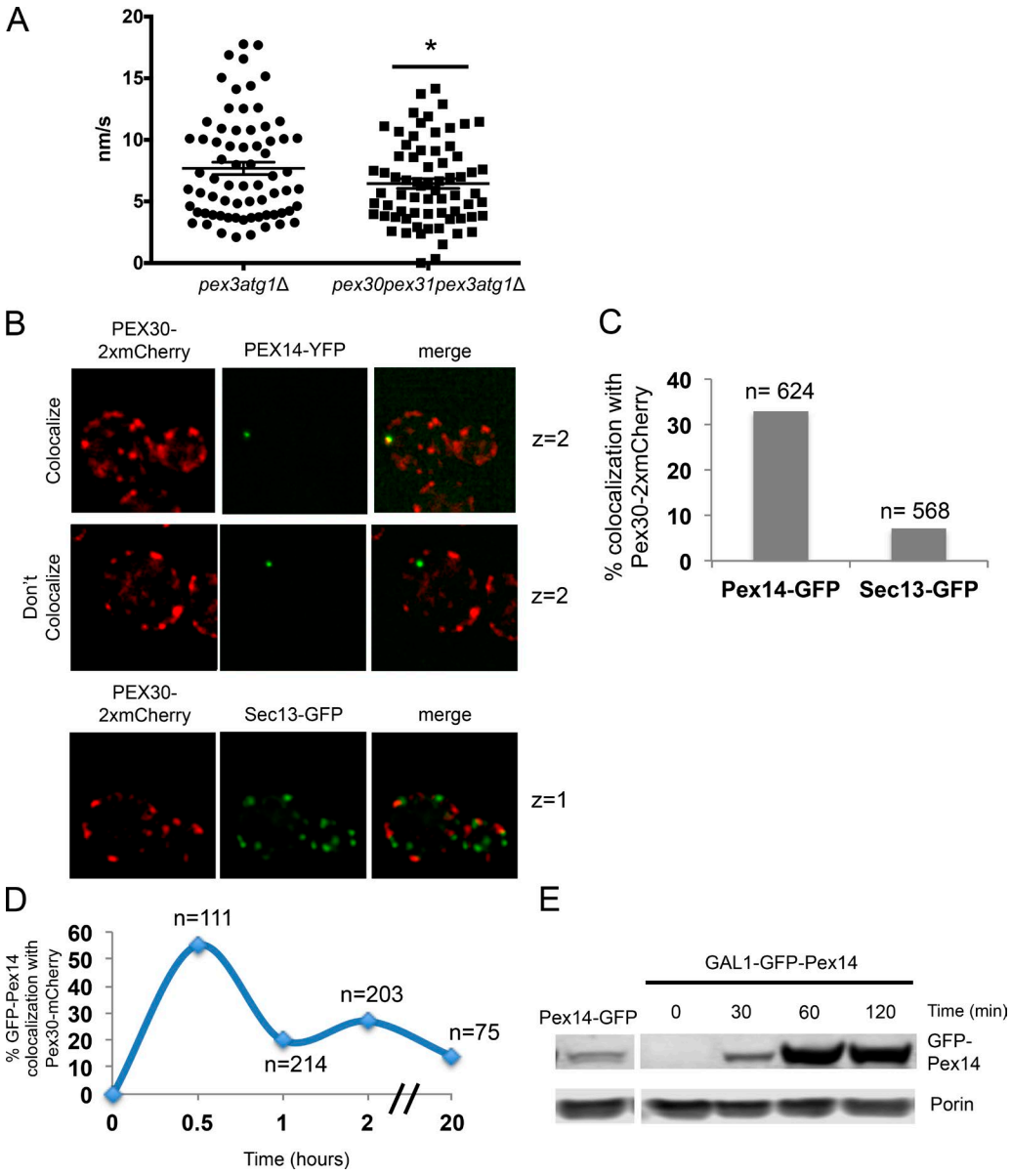

Figure 7. **Pex30-2xmCherry is enriched at sites of PPV production.** (A) Velocity of Pex14-GFP punctae; mean ± SE of 70 cells. *, $P < 0.05$. (B) Fluorescence microscopy images of *pex3atg1Δ* cells expressing endogenous Pex30-2xmCherry and either Pex14-YFP or Sec13-GFP. Stacks of three images with a step of size of 0.3 µm were taken and deconvolved; images from the indicated plane (z) are shown. (C) Quantification of experiment in B. *n*, number of Pex14-GFP or Sec13-GFP punctae. (D) Cells were grown as in Fig. 6 D, and stacks of three images with a step of size of 0.25 µm were taken at the indicated times and deconvolved. Images were used to quantify percent colocalization of GFP-Pex14 with Pex30-mCherry. *n*, number of GFP-Pex14 punctae counted. (E) Endogenous Pex14-GFP protein level of *pex3atg1Δ* cells grown in raffinose and protein level of GFP-Pex14 induced by galactose for 15 min and grown in raffinose for indicated time points.

ogy. Using EM, we found that deletion of *PEX30* and *PEX31* in *pex3atg1Δ* alters PPVs in two ways. First, most PPVs in *pex30pex31pex3atg1Δ* had about a twofold larger diameter than those in cells expressing Pex30p and Pex31p (Fig. 8, A, B [I], and C). Second, ∼27% of PPVs in cells lacking Pex30p and Pex31p form clusters of small vesicles close to the ER membrane (Fig. 8 B, II). Interestingly, overexpression of Pex30p not only increased the number of Pex14p-containing PPVs but also resulted in elongated PPVs (Fig. 8 D). Interestingly, overexpression of Pex30p does not elongate mature peroxisome in wild-type cells (unpublished data). The effect of Pex30p overexpression on PPV shape could be caused by a change in Pex30p localization. Using immunogold, we found that endogenously expressed Pex30p was exclusively on the ER and never on PPVs. However, in cells overexpressing Pex30p, a portion of the protein was found on PPVs together with Pex14-GFP (Fig. 8 D, II and III); the Pex30p in PPVs may contribute to their elongated shape. Collectively, these findings suggest that Pex30p might participate in shaping PPVs. However, whether membrane tubulation by Pex30p and Pex31p plays a role in regulating the morphology of PPVs remains to be investigated.

Discussion

In this study, we reveal that Pex30p and Pex31p are novel ER-shaping proteins that contain an N-terminal domain similar to the membrane curvature-stabilizing domains found in

Published November 8, 2016

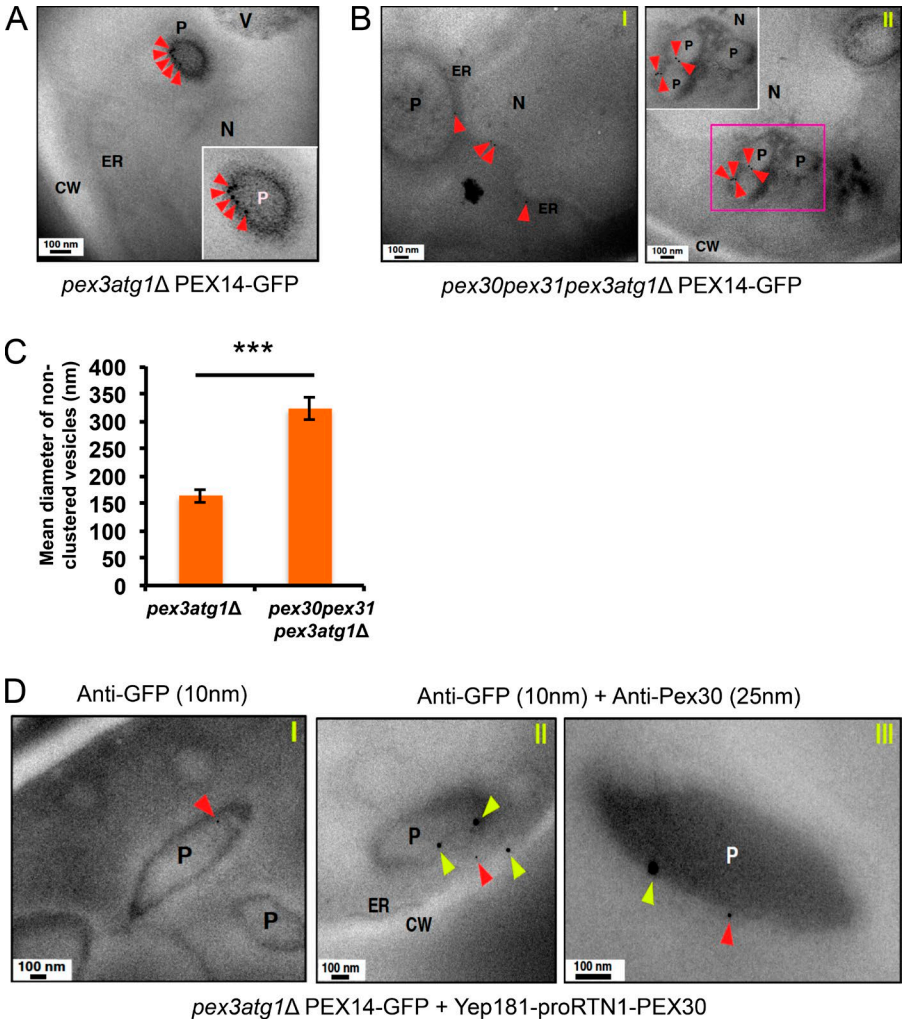

Figure 8. **Pex30p and Pex31p regulate the morphology of PPVs.** (A) Immunogold EM images of *pex3atg1Δ* cells expressing endogenous Pex14-GFP using anti-GFP antibodies. (B) As in A, except with *pex30pex31pex3atg1Δ* cells. Examples of two types of PPV morphology shown: large vesicles (I) and clustered vesicles (II). (C) Quantification of diameter of nonclustered PPVs identified by anti-GFP immuno-EM on cells expressing Pex14-GFP using anti-GFP antibody (mean ± SE in 20 cells; ***, $P < 0.005$). (D) Immunogold EM images of *pex3atg1Δ* cells expressing endogenous Pex14-GFP and overexpressing Pex30p using anti-GFP and anti-Pex30p antibodies (red arrowheads, Pex14-GFP; yellow arrowheads, Pex30p). CW, cell wall; N, nucleus; P, preperoxisomal vesicle; V, vacuole.

reticulons. We show that overexpression of Pex30p or Pex31p restores ER shape in *rtn1rtn2yop1Δ* cells (Fig. 1, C and D). Like the reticulons, Pex30p and Pex31p are localized mainly to ER tubules and the edges of ER sheets (Figs. 3 A and 4 A). However, Pex30p and Pex31p do not seem to shape the peripheral ER generally, as cells lacking these proteins have normal ER shape, and deletion of *PEX30* and *PEX31* in *yop1Δ* cells does not seem to exacerbate their ER morphology defect (Fig. S3). This is probably because Pex30p and Pex31p are much lower abundance proteins than the reticulons and Yop1p (Fig. 4 B), and it has previously been shown that the abundance of reticulons and reticulon-like proteins determines the extent of ER tubulation (Shibata et al., 2010). In fact, we show that Pex30p when expressed endogenously is present only at subdomains of the ER as opposed to the entire peripheral ER like the reticulon proteins (Fig. 4 A). Interestingly, we found that Rtn1p is depleted from the portions of the ER enriched in Pex30p (Fig. 4 C), suggesting that Pex30p may be the primary reticulon-like protein in these regions of the ER. Thus, we propose that Pex30p, and likely Pex31p, structure subdomains within the peripheral ER.

Our findings suggest that Pex30p localizes to domains in the ER where PPVs are generated. Pex30p and Pex31p are not required for PPV production, but the absence or overexpression of these proteins affects the size, shape, and number of PPVs (Fig. 5 C and Fig. 8, B–D). These findings are consistent with previous studies suggesting that Pex30p and Pex31p play roles in mature peroxisome biogenesis (Vizeacoumar et al., 2004). We propose that Pex30p and Pex31p help shape and generate ER subdomains involved in PPV biogenesis (Fig. 9). Although it is possible that Pex30p and Pex31p directly mediate peroxisome budding because they are membrane-shaping proteins, we favor the model that they help generate domains in which other proteins directly generate PPVs. Pex30p and Pex31p might help recruit proteins necessary for PPV production to these subdomains. The conserved DysF domain that is common to both Pex30p and Pex31p may interact with other proteins necessary for PPV production. Interestingly, Pex30p has previously been shown to interact with COPI components (David et al., 2013), which could play a role in PPV budding.

Pex30p forms many punctae in the ER, but there are only one to three Pex14-GFP punctae per cell (Figs. 4 A and 7 B), suggesting that Pex30-enriched ER domains may have functions in addition to PPV production. One function may be to promote close contacts between the ER and peroxisomes because previous studies have suggested that Pex30p plays a role in generating these contacts (David et al., 2013; Mast et al., 2016). Pex30-enriched ER domains could form contacts with other organelles as well.

Although we and others find that Pex30p is exclusively in the ER when cells are grown on glucose (Mast et al., 2016), previous studies have shown that a fraction of Pex30p localizes to peroxisomes when cells are grown with oleate or other

Published November 8, 2016

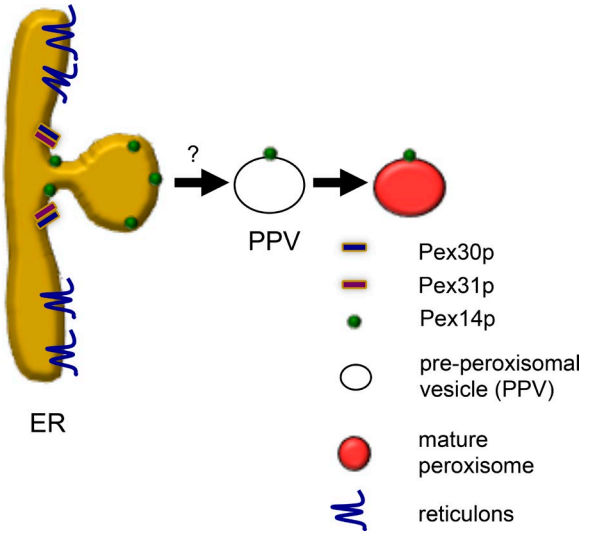

Figure 9. **Proposed model of PPV biogenesis from ER subdomains generated by Pex30p and Pex31p.**

conditions that induce peroxisome proliferation (Vizeacoumar et al., 2006; Yan et al., 2008). The function of Pex30p in mature peroxisome remains unclear. It may play a direct role in shaping peroxisome membranes; we find that when Pex30p is overexpressed, a fraction of the protein localizes to PPVs, and the shape of PPVs changes (Fig. 8 D).

Whether mammalian cells contain proteins like Pex30p and Pex31p that play roles in peroxisome biogenesis remains an open question. Although there are no obvious mammalian homologues of these proteins, it is possible that proteins with reticulon-like membrane-shaping domains could help generate discrete sites in the ER of mammalian cells where PPV are generated.

It seems likely that in both yeast and higher eukaryotes, there are several proteins that have reticulon-like domains that shape or form subdomains within the ER but do not affect bulk ER morphology. One such protein in yeast is Atg40p, a reticulon-like protein that probably helps form an ER subdomain degraded during ER-phagy (Mochida et al., 2015). The mammalian homologue of Atg40p, FAM134B, also has a reticulon-like domain (Khaminets et al., 2015). Interestingly, homology prediction using HHpred suggests that other proteins involved in peroxisome biogenesis, including Pex32p, Pex28p, and Pex29p, may also contain reticulon-like domains (Fig. S2). Thus, there may be several reticulon-like proteins that help form subdomains within the peripheral ER. It will be important to determine whether ER subdomains formed by novel reticulon-like proteins are structurally distinct from other regions of the peripheral ER. Such structural differences may help sort proteins into or exclude proteins from ER subdomains.

Materials and methods

Yeast strains and plasmids

The strains and plasmids used in this study are listed in Tables S1 and S2. Deletion strains were constructed by mating and/or PCR-based targeted homologous recombinations to replace the ORF of gene of interest with indicated cassettes (Longtine et al., 1998). The functional C-terminal tagged strains were also generated by PCR-based targeted homologous recombination. The 2xmCherry-URA3 and GFP-His3MX6 cassettes were obtained from O. Cohen-Fix (National Institutes of Health/National Institute of Diabetes and Digestive and Kidney Diseases, Bethesda, MD), YFP-KanMx6 from J. Cooper (National Institutes of Health/National Cancer Institute, Bethesda, MD), and yEmCherry-His5MX6 from J. Nunnari (University of California, Davis, Davis, CA). *TRP1-GAL1* and *TRP1-GAL1-GFP* cassettes (Longtine et al., 1998) were used to replace the promoters of *PEX3* and *PEX14*, respectively, to regulate the expression of these genes under galactose promoter.

Plasmids with the genes *PEX30*, *PEX31*, *PEX3*, *PEX32*, *PEX30 (W94C)*, *RTN2*, and *RTN2* (*W36C*) were individually cloned and expressed under strong *RTN1* promoter. The ORFs of these genes were fused to the *RTN1* promoter region (600 bp upstream of *RTN1*) and cloned into the BamHI–SalI site of Yeplac181 (a 2µ plasmid). The QuikChange II site-directed mutagenesis kit (Agilent Technologies) was used to create *PEX30* (W94C) and *RTN2* (W36C) cassettes. The *PEX30-GFP*, *PEX30 (1–235)-GFP*, and *PEX31-GFP* cassettes were expressed under their own promoters. The peroxisomal targeting sequence (SKL) was fused at the C terminus of the mCherry cassette expressed by the *GPD* promoter in the plasmid pRS425 (pRS425 was obtained from D. Goldfarb, University of Rochester, Rochester, NY). For the in vitro tubulation assay, the full-length coding region of Pex30p with an N-terminal 6xHis tag and a C-terminal Flag tag was PCR-amplified, cloned into the BamHI–XhoI site of pESC-URA (a 2µ plasmid), and overexpressed in the yeast strain FM135a.

Media and growth conditions

Cells with indicated plasmids were grown in synthetic complete (SC) media containing 0.67% yeast nitrogen base without amino acids (United States Biological) and an amino acid mix (United States Biological) containing 2% glucose, 2% raffinose, or 2% galactose. YPD medium (1% Bacto yeast extract, 2% Bacto Peptone, and 2% glucose) was also used to grow cells. All of the yeast cells were grown at 30°C.

Fluorescence microscopy

Cells were imaged live in growth media using a BX61 microscope (Olympus) with a UPlanAPO ×100/1.35 lens and a Retiga EX camera (QImaging) and processed using iVision software (version 4.0.5). For Fig. 4 A, Fig. 6 (A and D), and Fig. 7 B, imaging was performed at 27°C in an Environmental Chamber with a DeltaVision Spectris (Applied Precision Ltd.) comprising a wide-field inverted epifluorescence microscope (IX70; Olympus), a 100× NA 1.4 oil immersion objective (UPlanSAPO; Olympus), and a charge-coupled device CoolSnap HQ camera (Photometrics). For the time-lapse experiment, cells were spotted on a 30-µl solidified pad of 1% agarose prepared in SC media with raffinose. Time-lapse images were acquired every 4 min for 2 h for Fig. 6 D and every 2 min for 20 min for Fig. 7 A. Images were deconvolved (conserved ratio method) using SoftWorx (Applied Precision Ltd.). Brightness and contrast were adjusted using Photoshop CC (Adobe Systems).

Subcellular fractionation of peroxisomes

Subcellular fractionation was performed as described (Lam et al., 2010). In brief, cells were grown to OD_{550} of 1.0–1.5 in 20 ml SC medium followed by centrifugation at 4,000 *g* for 5 min. Cells were washed with sterile water, resuspended in softening medium (100 mM Tris, pH 9.4) and 10 mM DTT, and incubated for 15 min. Cells were centrifuged, and pellet was resuspended in spheroplast buffer (50 mM Hepes-KOH, pH 7.2, 1 M sorbitol, and 0.2% YPD) and digested with zymolyase-100T (20 µg/OD) at 30°C for 1 h. Spheroplasts were centrifuged at 4,000 *g* for 10 min at 4°C and resuspended in lysis buffer (20 mM Hepes-KOH,

Published November 8, 2016

pH 6.0, 0.25 M sorbitol, 0.15 M KOAc, and 1 mM $MgOAc_2$) with protease inhibitor mixture (Roche) and 1 mM PMSF. The suspension was homogenized in dounce homogenizer (Bellco Glass Inc.) with 20 strokes using a B pestle. The lysate was centrifuged at 4,000 *g* for 10 min. The postnuclear supernantant (300 µl) was loaded on the top of a Histodenz step gradient (2 ml; Sigma-Aldrich) ranging from 10 to 50% (400 µl: 50, 40, 30, and 20; 300 µl: 10%) followed by centrifugation for 2 h at 55,000 rpm at 4°C in a TLS-55 rotor (Beckman Coulter). Seven fractions were collected from the top, TCA precipitated, and analyzed by SDS-PAGE and immunoblotting.

EM

Sample preparation for EM was done as described previously (Choudhary et al., 2015), with some modifications. In brief, wild-type and mutant yeast cells were grown to mid-logarithmic growth phase, and cells corresponding to 10 OD_{600} units were centrifuged at 2,000 rpm for 5 min and fixed in 1 ml of fixative media (2.5% glutaraldehyde, 1.25% PFA, and 40 mM potassium phosphate, pH 7.0) for 20 min at RT. Cells were harvested, again resuspended in 1 ml fresh fixative media, and incubated on ice for 1 h. Cells were centrifuged and washed twice with 0.9% NaCl and once with water. Cells were incubated with 2% solution of $KMnO_4$ for 5 min at RT, centrifuged, and again resuspended with fresh solution of 2% $KMmO_4$ for 45 min at RT for en bloc staining. The cells were dehydrated using ethanol, embedded using Spurr's resin (Electron Microscopy Sciences), and polymerized as described previously (Choudhary et al., 2015). Semi- and ultrathin sections were produced with a diamond knife (DiATOME) on an ultra-microtome (Ultracut UCT; Leica Biosystems), collected on 200 mesh copper grids (Electron Microscopy Sciences), poststained with uranyl acetate and lead citrate, and visualized with a Tecnai T12 transmission electron microscope (FEI), operating at 120 kV. Pictures were recorded on a bottom-mounted 2k × 2k CCD camera (Gatan). Brightness and contrast were adjusted to the entire images using Photoshop (version CC 2014).

Immunogold EM

Exponentially growing yeast cells ∼10 OD_{600} units were fixed in a mixture of 1% glutaraldehyde, 2% PFA, and 0.03% picric acid (all from Electron Microscopy Sciences) in 0.1 M sodium cacodylate buffer, pH 7.4, for 15 min at RT. Cells were harvested, overlaid with fresh fixative, and incubated for 1 h on ice. Cells were centrifuged and washed twice with distilled water. Cells were resuspended in 1% tannic acid (Electron Microscopy Sciences) for 45 min at RT to enhance membrane contrast. Thereafter, cells were washed, treated with 1% sodium metaperiodate (15 min), followed by washing and incubation with 50 mM NH_4Cl (15 min), and again washed twice with water. Samples were overlaid with 1% aqueous uranyl acetate (Electron Microscopy Sciences) for 30 min at RT and washed with water. Samples were dehydrated using ethanol, embedded using LR white resin (Polysciences Inc.), and polymerized as described previously (Choudhary et al., 2015). Blocks were sectioned, and ultrathin sections (80 nm) were collected onto 200 mesh carbon-coated formvar nickel grids (Electron Microscopy Sciences). Immunolabeling was performed using mouse monoclonal anti-GFP antiserum (Roche) and rabbit anti–Pex30 antiserum (generated against 509–519 aa peptide of Pex30p by Yenzyme antibodies) followed by goat anti–mouse (10 nm), and goat anti–rabbit (25 nm)–conjugated protein A nanogold (Electron Microscopy Sciences) as per the manufacturer's instructions. Sections were briefly poststained with aqueous uranyl acetate and lead citrate and visualized with a Tecnai T12 transmission electron microscope (FEI), operating at 120 kV. Pictures were recorded on a bottom-mounted 2k × 2k CCD camera (Gatan). Brightness and contrast were adjusted to the entire images using Photoshop, version CC 2014 (Adobe Systems). For quantification, a gold particle was assigned to a compartment if it was within 25 nm of the limiting membrane or cytoplasm. Statistics were performed using two-tailed Student's *t* test.

Image quantification

The percent of cortical ER was determined from images of cells expressing ss-RFP-HDEL and Rtn1-GFP. Quantification was done as described (Shibata et al., 2010). In brief, images were thresholded above background, and the percentage of sheet area was calculated for each cell as the percentage of area of ss-RFP-HDEL that did not overlap with Rtn1-GFP using Metamorph software (Molecular Devices). Means and standard errors were calculated using Excel (Microsoft).

Assay for de novo biogenesis of peroxisomes

The assay was performed as described (David et al., 2013). Cells were grown in SC media containing 2% raffinose to mid logarithmic phase, washed twice with water, and shifted to SC media containing 2% galactose to induce expression of *PEX3*. Cells were examined for peroxisome formation at 2, 4, 6, and 8 h after induction.

In vitro tubulation

FM135a cells were transformed with the plasmids expressing Pex30p, grown in SC-URA with 2% glucose to OD_{600} nm of ∼1, induced by addition of 2% galactose to the medium, and then grown for 8 h. The cells were resuspended in TKG buffer (50 mM Tris, pH 7.5, 150 mM KCl, and 5% glycerol) and broken by high-pressure cell disrupter. The lysates were centrifuged at 500 *g* for 5 min to remove unbroken cells and then at 42,000 rpm in a Type 45 Ti rotor (Beckman Coulter) for 1 h to sediment the membranes. The membranes were solubilized in TKG plus 1% LDAO (Anatrace) for 1 h at 4°C, and insoluble materials were removed by centrifugation at 42,000 rpm for 0.5 h. His-Pex30p-Flag was isolated by a Ni-NTA column and further purified by gel filtration (Superdex-200; GE Healthcare) in TKG plus 0.05% LDAO. Purified Pex30 was concentrated to ∼1 mg/ml (Amicon Ultra; EMD Millipore).

Reconstitution

Chloroform-solubilized EPL were dried under a stream of N_2 gas followed by further drying in a spinning vacuum for 30 min. The lipid films were then dissolved in TK buffer (50 mM Tris, pH 7.5, and 150 mM KCl) plus 0.1% LDAO. Both protein and EPL were mixed to a final concentration of 0.2 mg/ml with a final volume of 100 µl. Protein and lipids were incubated for 1 h at RT. To remove the detergent, 5 µg Bio-Beads (Bio-Rad Laboratories) was added every hour, up to 4 h, under stirring. All reconstitutions were carried at RT.

Negative staining and EM

Negative staining was done with 2% uranyl acetate solubilized in deionized water. A drop of 5 µl sample solution was placed onto a glow-discharged carbon-coated copper grid for 1 min. Excessive sample was blotted off by filter paper, and the grids were washed with one drop of deionized water and stained with one drop of 2% uranyl acetate for 40 s. Images were collected at RT using an HT7700 transmission electron microscope (Hitachi) operated at an acceleration voltage of 80 kV.

Sucrose-gradient centrifugation

For sucrose-gradient centrifugation of reconstituted Pex30p, 20 µl reconstitution mix was applied to a four-step sucrose gradient (20, 30, 40, and 50%, 0.5 ml each). Centrifugation was performed at 55,000 rpm in a TLS-55 rotor (Beckman Coulter) for 2 h at 25°C. Fractions (∼0.2 ml) were collected from the top and analyzed by SDS-PAGE and immunoblotting. To follow lipid distribution after the gradient, 1% of 1,2-dipalmitoyl-snglycero-3-phosphoethanolamine-*N*-(7-nitro-

2-1,3-benzoxadiazol-4-yl; 16:0 NBD-PE) was mixed into the EPL. The fluorescence intensity of NBD was monitored using a microplate reader (Synergy 4; BioTek) with an excitation of 460 nm and emission of 538 nm. The amount of Pex30p-Flag in each fraction was detected by immunoblotting, in comparison to purified Pex30p-Flag in LDAO subjected to a same gradient. The amount of lipids in each fraction was estimated from the percentage of the total fluorescence.

Protein extraction and Western blot analysis

Proteins were extracted from cells grown to an OD_{550} of 1.0, separated by 4–12% SDS-PAGE (Invitrogen), transferred to nitrocellulose membrane, and analyzed using primary antibodies to GFP (1:1,000; Invitrogen), Dpm1p (1:500; Thermo Fisher Scientific), Pex3p (1:1,000; provided by R. Erdmann, Ruhr University, Bochum, Germany), and Porin (1:1,000; Invitrogen). Proteins were visualized using appropriate IRDye secondary antibody (LI-COR Biosciences; 1:10,000) followed by detection using the Odyssey system.

Measuring PPV movement

The *pex3atg1Δ* and *pex30pex31pex3atg1Δ* mutant cells expressing endogenously tagged Pex14-GFP were grown to mid-logarithmic growth phase. Time-lapse images were acquired every 2 min for 20 min. A stack of 20 images with a step size of 0.25 µm was acquired at each time point. Images in each stack were combined into a 2D image using the maximum intensity projection setting. The total distance traveled by Pex14-GFP was measured using SoftWorx (Applied Precision Ltd.) and divided by total time to give velocity (nanometers per second). Mean and standard error (SE) were calculated from data obtained from at least 70 cells using Prism 6 (GraphPad Software).

Online supplemental material

Fig. S1 shows the effect of PEX30 or PEX31 overexpression on total lipid phosphate per cell of *spo7Δ* cells (Bartlett, 1959). Fig. S2 shows the reticulon-like domain in Pex proteins identified using the structure-based homology prediction program HHpred. Fig. S3 shows that ER morphology is not altered in strains lacking Pex30p and Pex31p. Fig. S4 shows representative images of cells used to generate the graph in Fig. 5 A. Fig. S5 shows that Pex13p-mCherry and Pex14-GFP colocalize in *pex3atg1Δ* cells. Video 1 shows that nascent GFP-Pex14 puncta originate on the ER membrane and subsequently move away from the ER. Tables S1 and S2 contain the strains and plasmids, respectively, used in this study.

Acknowledgments

The authors thank Alexandre Toulmay for technical assistance and valuable discussions, Yihong Ye for critically reading the manuscript, and Julia Cooper for sharing the DeltaVision microscope facility.

This work was supported by the Intramural Research Program of the National Institute of Diabetes and Digestive and Kidney Diseases. J. Hu was supported by the National Natural Science Foundation of China (grant 31225006) and an International Early Career Scientist grant from Howard Hughes Medical Institute. T.P. Levine's laboratory was supported by the Biotechnology and Biological Sciences Research Council Bioinformatics and Biological Resources Fund (grant BB/M011801). V. Choudhary was supported by a fellowship from Schweizerischer Nationalfonds zur Förderung der Wissenschaftlichen Forschung (grants PA00P3_145358 and P300P3_158454).

The authors declare no competing financial interests.

Submitted: 17 February 2016
Revised: 29 July 2016
Accepted: 21 October 2016

References

Agrawal, G., and S. Subramani. 2016. De novo peroxisome biogenesis: Evolving concepts and conundrums. *Biochim. Biophys. Acta.* 1863:892–901. http://dx.doi.org/10.1016/j.bbamcr.2015.09.014

Agrawal, G., S. Joshi, and S. Subramani. 2011. Cell-free sorting of peroxisomal membrane proteins from the endoplasmic reticulum. *Proc. Natl. Acad. Sci. USA.* 108:9113–9118. http://dx.doi.org/10.1073/pnas.1018749108

Agrawal, G., S.N. Fassas, Z.J. Xia, and S. Subramani. 2016. Distinct requirements for intra-ER sorting and budding of peroxisomal membrane proteins from the ER. *J. Cell Biol.* 212:335–348. http://dx.doi.org/10.1083/jcb.201506141

Anwar, K., R.W. Klemm, A. Condon, K.N. Severin, M. Zhang, R. Ghirlando, J. Hu, T.A. Rapoport, and W.A. Prinz. 2012. The dynamin-like GTPase Sey1p mediates homotypic ER fusion in *S. cerevisiae*. *J. Cell Biol.* 197:209–217. http://dx.doi.org/10.1083/jcb.201111115

Bartlett, G.R. 1959. Phosphorus assay in column chromatography. *J. Biol. Chem.* 234:466–468.

Bellu, A.R., F.A. Salomons, J.A. Kiel, M. Veenhuis, and I.J. Van Der Klei. 2002. Removal of Pex3p is an important initial stage in selective peroxisome degradation in *Hansenula polymorpha*. *J. Biol. Chem.* 277:42875–42880. http://dx.doi.org/10.1074/jbc.M205437200

Campbell, J.L., A. Lorenz, K.L. Witkin, T. Hays, J. Loidl, and O. Cohen-Fix. 2006. Yeast nuclear envelope subdomains with distinct abilities to resist membrane expansion. *Mol. Biol. Cell.* 17:1768–1778. http://dx.doi.org/10.1091/mbc.E05-09-0839

Chen, S., P. Novick, and S. Ferro-Novick. 2012. ER network formation requires a balance of the dynamin-like GTPase Sey1p and the Lunapark family member Lnp1p. *Nat. Cell Biol.* 14:707–716. http://dx.doi.org/10.1038/ncb2523

Chen, S., T. Desai, J.A. McNew, P. Gerard, P.J. Novick, and S. Ferro-Novick. 2015. Lunapark stabilizes nascent three-way junctions in the endoplasmic reticulum. *Proc. Natl. Acad. Sci. USA.* 112:418–423. http://dx.doi.org/10.1073/pnas.1423026112

Choudhary, V., N. Ojha, A. Golden, and W.A. Prinz. 2015. A conserved family of proteins facilitates nascent lipid droplet budding from the ER. *J. Cell Biol.* 211:261–271. http://dx.doi.org/10.1083/jcb.201505067

David, C., J. Koch, S. Oeljeklaus, A. Laernsack, S. Melchior, S. Wiese, A. Schummer, R. Erdmann, B. Warscheid, and C. Brocard. 2013. A combined approach of quantitative interaction proteomics and live-cell imaging reveals a regulatory role for endoplasmic reticulum (ER) reticulon homology proteins in peroxisome biogenesis. *Mol. Cell. Proteomics.* 12:2408–2425. http://dx.doi.org/10.1074/mcp.M112.017830

Dawson, T.R., M.D. Lazarus, M.W. Hetzer, and S.R. Wente. 2009. ER membrane-bending proteins are necessary for de novo nuclear pore formation. *J. Cell Biol.* 184:659–675. http://dx.doi.org/10.1083/jcb.200806174

Dimitrov, L., S.K. Lam, and R. Schekman. 2013. The role of the endoplasmic reticulum in peroxisome biogenesis. *Cold Spring Harb. Perspect. Biol.* 5:a013243. http://dx.doi.org/10.1101/cshperspect.a013243

English, A.R., and G.K. Voeltz. 2013. Rab10 GTPase regulates ER dynamics and morphology. *Nat. Cell Biol.* 15:169–178. http://dx.doi.org/10.1038/ncb2647

Goyal, U., and C. Blackstone. 2013. Untangling the web: mechanisms underlying ER network formation. *Biochim. Biophys. Acta.* 1833:2492–2498. http://dx.doi.org/10.1016/j.bbamcr.2013.04.009

Haan, G.J., R.J. Baerends, A.M. Krikken, M. Otzen, M. Veenhuis, and I.J. van der Klei. 2006. Reassembly of peroxisomes in *Hansenula polymorpha* pex3 cells on reintroduction of Pex3p involves the nuclear envelope. *FEMS Yeast Res.* 6:186–194. http://dx.doi.org/10.1111/j.1567-1364.2006.00037.x

Hoepfner, D., D. Schildknegt, I. Braakman, P. Philippsen, and H.F. Tabak. 2005. Contribution of the endoplasmic reticulum to peroxisome formation. *Cell.* 122:85–95. http://dx.doi.org/10.1016/j.cell.2005.04.025

Hu, J., Y. Shibata, C. Voss, T. Shemesh, Z. Li, M. Coughlin, M.M. Kozlov, T.A. Rapoport, and W.A. Prinz. 2008. Membrane proteins of the endoplasmic reticulum induce high-curvature tubules. *Science.* 319:1247–1250. http://dx.doi.org/10.1126/science.1153634

Hu, J., Y. Shibata, P.P. Zhu, C. Voss, N. Rismanchi, W.A. Prinz, T.A. Rapoport, and C. Blackstone. 2009. A class of dynamin-like GTPases involved in the generation of the tubular ER network. *Cell.* 138:549–561. http://dx.doi.org/10.1016/j.cell.2009.05.025

Khaminets, A., T. Heinrich, M. Mari, P. Grumati, A.K. Huebner, M. Akutsu, L. Liebmann, A. Stolz, S. Nietzsche, N. Koch, et al. 2015. Regulation of endoplasmic reticulum turnover by selective autophagy. *Nature.* 522:354–358. http://dx.doi.org/10.1038/nature14498

Kim, P.K., R.T. Mullen, U. Schumann, and J. Lippincott-Schwartz. 2006. The origin and maintenance of mammalian peroxisomes involves a de novo PEX16-dependent pathway from the ER. *J. Cell Biol.* 173:521–532. http://dx.doi.org/10.1083/jcb.200601036

Knoops, K., S. Manivannan, M.N. Cepinska, A.M. Krikken, A.M. Kram, M. Veenhuis, and I.J. van der Klei. 2014. Preperoxisomal vesicles can form in the absence of Pex3. *J. Cell Biol.* 204:659–668. http://dx.doi.org/10.1083/jcb.201310148

Lam, S.K., N. Yoda, and R. Schekman. 2010. A vesicle carrier that mediates peroxisome protein traffic from the endoplasmic reticulum. *Proc. Natl. Acad. Sci. USA.* 107:21523–21528. http://dx.doi.org/10.1073/pnas.1013397107

Longtine, M.S., A. McKenzie III, D.J. Demarini, N.G. Shah, A. Wach, A. Brachat, P. Philippsen, and J.R. Pringle. 1998. Additional modules for versatile and economical PCR-based gene deletion and modification in *Saccharomyces cerevisiae*. *Yeast.* 14:953–961. http://dx.doi.org/10.1002/(SICI)1097-0061(199807)14:10<953::AID-YEA293>3.0.CO;2-U

Mast, F.D., A. Jamakhandi, R.A. Saleem, D.J. Dilworth, R.S. Rogers, R.A. Rachubinski, and J.D. Aitchison. 2016. Peroxins Pex30 and Pex29 dynamically associate with reticulons to regulate peroxisome biogenesis from the endoplasmic reticulum. *J. Biol. Chem.* 291:15408–15427. http://dx.doi.org/10.1074/jbc.M116.728154

Mochida, K., Y. Oikawa, Y. Kimura, H. Kirisako, H. Hirano, Y. Ohsumi, and H. Nakatogawa. 2015. Receptor-mediated selective autophagy degrades the endoplasmic reticulum and the nucleus. *Nature.* 522:359–362. http://dx.doi.org/10.1038/nature14506

Motley, A.M., and E.H. Hettema. 2007. Yeast peroxisomes multiply by growth and division. *J. Cell Biol.* 178:399–410. http://dx.doi.org/10.1083/jcb.200702167

Rucktäschel, R., W. Girzalsky, and R. Erdmann. 2011. Protein import machineries of peroxisomes. *Biochim. Biophys. Acta.* 1808:892–900. http://dx.doi.org/10.1016/j.bbamem.2010.07.020

Santos-Rosa, H., J. Leung, N. Grimsey, S. Peak-Chew, and S. Siniossoglou. 2005. The yeast lipin Smp2 couples phospholipid biosynthesis to nuclear membrane growth. *EMBO J.* 24:1931–1941. http://dx.doi.org/10.1038/sj.emboj.7600672

Shemesh, T., R.W. Klemm, F.B. Romano, S. Wang, J. Vaughan, X. Zhuang, H. Tukachinsky, M.M. Kozlov, and T.A. Rapoport. 2014. A model for the generation and interconversion of ER morphologies. *Proc. Natl. Acad. Sci. USA.* 111:E5243–E5251. http://dx.doi.org/10.1073/pnas.1419997111

Shibata, Y., C. Voss, J.M. Rist, J. Hu, T.A. Rapoport, W.A. Prinz, and G.K. Voeltz. 2008. The reticulon and DP1/Yop1p proteins form immobile oligomers in the tubular endoplasmic reticulum. *J. Biol. Chem.* 283:18892–18904. http://dx.doi.org/10.1074/jbc.M800986200

Shibata, Y., T. Shemesh, W.A. Prinz, A.F. Palazzo, M.M. Kozlov, and T.A. Rapoport. 2010. Mechanisms determining the morphology of the peripheral ER. *Cell.* 143:774–788. http://dx.doi.org/10.1016/j.cell.2010.11.007

Shindiapina, P., and C. Barlowe. 2010. Requirements for transitional endoplasmic reticulum site structure and function in *Saccharomyces cerevisiae*. *Mol. Biol. Cell.* 21:1530–1545. http://dx.doi.org/10.1091/mbc.E09-07-0605

Tolley, N., I.A. Sparkes, P.R. Hunter, C.P. Craddock, J. Nuttall, L.M. Roberts, C. Hawes, E. Pedrazzini, and L. Frigerio. 2008. Overexpression of a plant reticulon remodels the lumen of the cortical endoplasmic reticulum but does not perturb protein transport. *Traffic.* 9:94–102. http://dx.doi.org/10.1111/j.1600-0854.2007.00670.x

Ueda, H., E. Yokota, N. Kutsuna, T. Shimada, K. Tamura, T. Shimmen, S. Hasezawa, V.V. Dolja, and I. Hara-Nishimura. 2010. Myosin-dependent endoplasmic reticulum motility and F-actin organization in plant cells. *Proc. Natl. Acad. Sci. USA.* 107:6894–6899. http://dx.doi.org/10.1073/pnas.0911482107

van der Zand, A., I. Braakman, and H.F. Tabak. 2010. Peroxisomal membrane proteins insert into the endoplasmic reticulum. *Mol. Biol. Cell.* 21:2057–2065. http://dx.doi.org/10.1091/mbc.E10-02-0082

Van Veldhoven, P.P. 2010. Biochemistry and genetics of inherited disorders of peroxisomal fatty acid metabolism. *J. Lipid Res.* 51:2863–2895. http://dx.doi.org/10.1194/jlr.R005959

Vedrenne, C., D.R. Klopfenstein, and H.P. Hauri. 2005. Phosphorylation controls CLIMP-63-mediated anchoring of the endoplasmic reticulum to microtubules. *Mol. Biol. Cell.* 16:1928–1937. http://dx.doi.org/10.1091/mbc.E04-07-0554

Vizeacoumar, F.J., J.C. Torres-Guzman, D. Bouard, J.D. Aitchison, and R.A. Rachubinski. 2004. Pex30p, Pex31p, and Pex32p form a family of peroxisomal integral membrane proteins regulating peroxisome size and number in *Saccharomyces cerevisiae*. *Mol. Biol. Cell.* 15:665–677. http://dx.doi.org/10.1091/mbc.E03-09-0681

Vizeacoumar, F.J., W.N. Vreden, J.D. Aitchison, and R.A. Rachubinski. 2006. Pex19p binds Pex30p and Pex32p at regions required for their peroxisomal localization but separate from their peroxisomal targeting signals. *J. Biol. Chem.* 281:14805–14812. http://dx.doi.org/10.1074/jbc.M601808200

Voeltz, G.K., W.A. Prinz, Y. Shibata, J.M. Rist, and T.A. Rapoport. 2006. A class of membrane proteins shaping the tubular endoplasmic reticulum. *Cell.* 124:573–586. http://dx.doi.org/10.1016/j.cell.2005.11.047

Voss, C., S. Lahiri, B.P. Young, C.J. Loewen, and W.A. Prinz. 2012. ER-shaping proteins facilitate lipid exchange between the ER and mitochondria in *S. cerevisiae*. *J. Cell Sci.* 125:4791–4799. http://dx.doi.org/10.1242/jcs.105635

Waterman-Storer, C.M., and E.D. Salmon. 1998. Endoplasmic reticulum membrane tubules are distributed by microtubules in living cells using three distinct mechanisms. *Curr. Biol.* 8:798–806. http://dx.doi.org/10.1016/S0960-9822(98)70321-5

West, M., N. Zurek, A. Hoenger, and G.K. Voeltz. 2011. A 3D analysis of yeast ER structure reveals how ER domains are organized by membrane curvature. *J. Cell Biol.* 193:333–346. http://dx.doi.org/10.1083/jcb.201011039

Westrate, L.M., J.E. Lee, W.A. Prinz, and G.K. Voeltz. 2015. Form follows function: The importance of endoplasmic reticulum shape. *Annu. Rev. Biochem.* 84:791–811. http://dx.doi.org/10.1146/annurev-biochem-072711-163501

Williams, C., and I.J. van der Klei. 2013. Pexophagy-linked degradation of the peroxisomal membrane protein Pex3p involves the ubiquitin-proteasome system. *Biochem. Biophys. Res. Commun.* 438:395–401. http://dx.doi.org/10.1016/j.bbrc.2013.07.086

Witkin, K.L., Y. Chong, S. Shao, M.T. Webster, S. Lahiri, A.D. Walters, B. Lee, J.L. Koh, W.A. Prinz, B.J. Andrews, and O. Cohen-Fix. 2012. The budding yeast nuclear envelope adjacent to the nucleolus serves as a membrane sink during mitotic delay. *Curr. Biol.* 22:1128–1133. http://dx.doi.org/10.1016/j.cub.2012.04.022

Yan, M., D.A. Rachubinski, S. Joshi, R.A. Rachubinski, and S. Subramani. 2008. Dysferlin domain-containing proteins, Pex30p and Pex31p, localized to two compartments, control the number and size of oleate-induced peroxisomes in *Pichia pastoris*. *Mol. Biol. Cell.* 19:885–898. http://dx.doi.org/10.1091/mbc.E07-10-1042

Yonekawa, S., A. Furuno, T. Baba, Y. Fujiki, Y. Ogasawara, A. Yamamoto, M. Tagaya, and K. Tani. 2011. Sec16B is involved in the endoplasmic reticulum export of the peroxisomal membrane biogenesis factor peroxin 16 (Pex16) in mammalian cells. *Proc. Natl. Acad. Sci. USA.* 108:12746–12751. http://dx.doi.org/10.1073/pnas.1103283108